THERMAL-MECHANICAL MODELLING OF LAMINATES WITH FIRE PROTECTION COATING

A.P. Mouritz[*1], S. Feih[1], E. Kandare[1] & A.G. Gibson[2]

1. School of Aerospace, Mechanical & Manufacturing Engineering, RMIT University, GPO Box 2476, Melbourne, Victoria, 3001, Australia

2. Centre for Composite Materials Engineering, Stephenson Building, University of Newcastle, Newcastle NE1 7RU, England

ABSTRACT

This paper presents a modelling approach to analyse the protection provided by passive and intumescent surface coatings on glass fibre reinforced laminate substrates exposed to fire. The modelling involves a multi-stage analytical approach: (i) thermal analysis of heat transfer from the fire through the surface insulation coating, which includes decomposition and expansion in the case of an intumescent material; (ii) thermal-chemical analysis of heat transfer through the fibreglass laminate substrate (beneath the fire protective coating), including decomposition of the polymer matrix; and (iii) thermal-mechanical analysis of softening and failure of the laminate under in-plane tension or compression loading. The modelling approach is validated using experimental temperature and strength data from fire structural tests performed on woven glass-vinyl ester laminates insulated with passive (ceramic fibre mat) or organic intumescent surface coatings.

Keywords:

A. Polymer-matrix composites (PMCs); B. High-temperature properties; C. Analytical modelling; Fire

1 INTRODUCTION

A long standing concern with the use of fibre-polymer composite materials in load-bearing structures is softening and failure when exposed to fire. The polymer matrix phase of most structural composite materials will soften (~150^{o}C) and decompose (~300-400^{o}C) at temperatures well below that of most hydrocarbon fires, where the temperature at the flame core can exceed 1200^{o}C. The structural survivability of composites in fire relies on the material resisting heat-induced softening, deformation, damage and failure; rather than on the avoidance of flaming combustion. Numerous research studies have theoretically and/or experimentally investigated the reduction to the mechanical properties and the failure strength of composites when exposed directly to fire [1-17].

The softening and failure of composite materials at temperatures lower than the flame temperature of cellulosic (e.g. wood) fires (approximately 900^{o}C), hydrocarbon fires (1200-1400^{o}C) and most other types of fire means it is sometimes necessary to protect structures using an insulation coating. Coatings are broadly classified as passive or active systems. Passive coatings are insulating materials with low thermal conductivity and are physically and chemically inert when exposed to high temperature. These coatings work by slowing heat flow

[*] Corresponding author.
Email: adrian.mouritz@rmit.edu.au
Tel: +61 3 9225 6269
Fax: +61 3 9225 6108

from the fire into the composite substrate, and commercial examples include mineral fibre mats and cement-based materials. Active coatings work by undergoing chemical and/or physical changes when heated by fire resulting in the lowering of the flame temperature or insulation of the composite, and the most used active coatings are organic intumescent systems. Both passive and active coatings are used to slow heat conduction from the fire into the underlying composite substrate, and thereby delay the onset and rate of softening, and consequently improve the fire resistance and survivability of composite structures. The coatings are also used to resist flame spread and to extend the time to flashover by slowing the heat-up rate and decomposition rate of the composite material.

Improvements to the fire reaction properties of composites when insulated with a passive or intumescent coating, such as increased time-to-ignition, reduced flame spread rate and lower heat release rate, are well known [see work cited in 18]. Information is also available on the residual post-fire mechanical properties of composites protected with passive or intumescent coatings [e.g. 19,20]. However, much less information is available on the structural performance of composites with insulation coatings during fire exposure. That is, the capacity of passive or intumescent coatings to improve the fire structural survivability of composites is not well understood.

Models to predict the improvement to the fire resistance of composites protected with surface coatings are lacking. Such models are required to minimise the need for fire structural tests which are currently used to assess the efficacy of coating systems, because (among other reasons) such tests are expensive and time-consuming. Furthermore, the test results are usually only valid for the specific fire test condition, and cannot be used to assess the performance of coatings under different fire conditions. A model which can accurately predict the protection provided by any type of passive or intumescent coating offers the possibility of screening and selecting insulation materials that provide the best protection for different fire conditions without the need for an extensive series of experimental fire tests.

This paper presents a modelling approach to calculate the level of structural protection offered by passive or intumescent coatings to fibreglass laminate structures. The approach consists of a coupled three-stage analytical solution: (1) analysis of heat transfer through the coating system when heated by fire, which is then used for the (2) analysis of heat transfer and decomposition in the laminate substrate, which is then used for the (3) analysis of softening and failure of the laminate under compression or tension loading.

The novelty of this approach is the coupling of existing models for heat transfer through passive coating or intumescent coatings with models for predicting the temperature, decomposition, softening and failure of laminates without coatings developed by the authors and their colleagues [10-12]. The coupling of the separate models and the experimental assessment of the numerical accuracy of the modelling approach is the original aspect of the work presented in this paper. In addition, the paper aims to quantify the numerical accuracy of the thermal and mechanical components to the models to the prediction of the failure temperature and failure time of insulated laminates.

It is envisaged that this modelling approach can be used to optimise the design and material selection of fire protection coating systems for fibreglass laminates used in high fire risk structural applications, and thereby limit the need for fire structural tests. It should be noted that the analysis presented in this paper is specific to polymer matrix laminates reinforced with continuous glass fibres. It is possible to modify the model to analyse laminates containing thermally reactive fibre reinforcement, such as carbon or aramid. However, the modelling of laminates reinforced with fibres other than glass is beyond the scope of this paper.

2 MODEL FOR FIBREGLASS LAMINATES WITH FIRE PROTECTIVE COATING

The model used to analyse the fire structural response of fibreglass laminates protected with a passive or intumescent surface coating involves a coupled three-step analytical solution which involves the following.

(1) Analysis of heat transfer through the coating when heated from one side by fire. Heat transfer through the passive coating is analysed using heat conduction theory. Heat transfer through the intumescent coating is analysed using heat conduction theory, chemical decomposition kinetics of the active compounds in the coating system, and the volumetric swelling effect of the coating due to the intumescent reaction process.

(2) Analysis of heat transfer and decomposition of the fibreglass laminate substrate due to heat conduction from the fire via the coating system. The analysis determines the temperature rise at any location in the laminate as well as calculates the mass loss (due to decomposition) of the polymer matrix phase.

(3) Analysis of softening and failure of the fibreglass laminate. The analysis calculates the reduction in strength resulting from thermal softening and decomposition of the laminate. The analysis estimates the failure temperature and time of the laminate under in-plane tension and compression loading.

Figure 1 presents a flowchart that out-lines the major steps involved in the analysis. Included in the steps is a listing of the calculated out-puts (e.g. temperature, mass loss) and the required thermal and material input data (e.g. heat flux/temperature of fire, thermal conductivity of laminate). Analysis of the passive coating assumes that this material is inert in fire whereas analysis of the intumescent coating assumes it reacts and swells when heated by fire. Due to their different responses to fire, the analysis of the two coating systems must be different, as indicated in figure 1. Following this first step in the analysis, the second and third steps of the model involving the fibreglass laminate are independent of the type of coating system.

The model assumes that one side of a flat fibreglass-polymer panel protected with a passive or intumescent coating is heated at a constant heat flux radiated by fire, as represented in figure 2. During fire attack it is assumed the laminate is supporting a constant compression or tension load. It is also assumed that the entire applied load is supported by the laminate and that the coating system is non-structural and therefore does not have load-bearing capacity.

The model does not analyse the combustion process and heat dynamics of the fire. The effects of flame turbulence, flame impingement and flame spread are also not considered in the analysis. However, the modelling approach can be modified to consider these effects by coupling a flame model based on computational fluid mechanics and combustion theory [e.g. 21,22] with the thermal-mechanical model for the material system presented in this paper. Instead, it is assumed that the passive and intumescent coatings are evenly heated over their entire surface at a net heat flux (q) which is determined by:

$$q = \varepsilon_f \sigma^* T_f^4 - \varepsilon_c \sigma^* T_s^4 + h_{fc}(T_f - T_c) \qquad [1]$$

The first term on the right-hand side is the heat flux radiated from the fire, the second term is the heat loss from the coating surface due to radiation, and the third term is the convective heat transfer between the fire and coating surface. The subscripts f and c refer to the fire and coating surface, respectively. ε is the emissivity, σ^* is the Stefan-Boltzman constant, h_{fc} is the

convection heat transfer coefficient at the fire/coating boundary, and *T* is the absolute temperature.

Modelling of Coating System

Modelling of Passive Coating

This section describes the analysis used to calculate the heat transfer through a passive coating when exposed to one-sided radiant heating from fire. Assuming that the insulation material does not decompose or undergo a phase change, then heat transfer through the coating can be modelled using heat conduction theory. The temperature rise in the coating with increased exposure time to the radiant heat flux of the fire is calculated using the one-dimensional heat conduction equation:

$$\left[\frac{\partial T}{\partial t}\right]_{pc} = \frac{\left[\frac{\partial}{\partial x}\left(k_x^{pc}(T)\frac{\partial T}{\partial x}\right)\right]}{\left[\rho_{pc}.C_p^{pc}(T)\right]} \qquad [2]$$

where the subscript/superscript *pc* refers to passive coating. *T* is the temperature and *t* is the heating time. *x* refers to the through-thickness direction of the material system. k^{pc} is the thermal conductivity and C_p^{pc} is the specific heat capacity of the passive coating material, and both these properties are assumed to be isotropic and dependent on the temperature. The temperature dependency of k^{pc} and C_p^{pc} cannot be calculated, and must be determined experimentally between ambient temperature (~20^{o}C) and the maximum temperature reached by the coating during fire exposure. ρ_{pc} is the bulk density of the coating material.

To solve Eqn. 2, a predefined heating condition (temperature-heating time curve) is imposed on the front surface (at $x = 0$) of the passive coating. This condition can be a standard heating curve used for the fire qualification testing of materials (e.g. ASTM E119 cellulosic fire curve or UL1709 hydrocarbon fire curve) or it can be a non-standard curve. Heat transfer through the coating is solved using a forward finite difference (FFD) method. In this method, Eqn. 2 is solved at different spatial through-thickness locations for increasing increments of heating time starting at $t = 0$. A constant time step increment is used between successive analytical iterations. Using this FFD method the heat conduction through the passive coating for increasing exposure time to the surface heat flux is calculated.

Modelling of Intumescent Coating System

Modelling heat transfer through an intumescent coating is more complicated than a passive coating because the active compounds in the intumescent material cause it to decompose and swell into a thick, porous carbonaceous char. The chemical and physical changes to the intumescent coating have a significant influence on heat conduction. Modelling of heat transfer through an organic intumescent surface coating is based on the recent analysis by Griffin [23]. The model calculates the temperature rise in the coating with increasing fire exposure time due to three thermal effects: heat conduction; heat evolved (or absorbed) due to reaction of the active compounds in the intumescent material; and convective heat flow of volatile gases generated by the reactions which diffuse from the coating into the fire.

The net heat flux at the intumescent coating surface is determined by Eqn 1. It is assumed that the surface emissivity (ε_c) is unchanged despite the coating decomposing into a carbonaceous material due to the reaction processes. The temperature rise of the intumescent coating is calculated using [23]:

$$\left[\frac{\partial T}{\partial t}\right]_{ic} = \frac{\left\{\left[\frac{\partial}{\partial x}\left(k_c^{ic}(T)\frac{\partial T}{\partial x}\right)\right] + \Delta h_{ic}\right\}}{\left[\rho_{ic}(T).C_p^{ic}(T)\right]} \quad [3]$$

The first term on the right hand side of the numerator relates to heat conduction in the through-thickness direction of the intumescent coating. The subscript/superscript *ic* refers to intumescent coating. The thermal conductivity (k^{ic}) and specific heat capacity (C_p^{ic}) of the intumescent coating are assumed to be isotropic and temperature-dependent, and these thermal properties must be experimentally measured. ρ_{ic} is the coating density and is a temperature-dependent property due to mass loss caused by the intumescent reaction process. The second term (Δh_{ic}) of the numerator is the net thermal energy resulting from the reaction process of the active compounds in the coating. This term combines the exothermic (or endothermic) energy from the chemical reactions of the active compounds with the energy due to mass flow of reaction volatiles through the coating towards the heated surface. Δh_{ic} is calculated using:

$$\Delta h_{ic} = \rho_0(1-\omega)\sum_k \gamma_k r_k \Delta h_k \quad [4]$$

where ρ_o is the initial density and ω is the void fraction of the intumescent coating. γ_k, r_k and h_k are the mass fraction, reaction rate and specific enthalpy of the active compound (designated type *k*) in the intumescent reaction process (which must be experimentally determined using thermo-gravimetric analysis, TGA).

The reaction rate of the active compound '*k*' in the intumescent coating is determined using the first-order Arrhenius rate equation:

$$r_k = \frac{\partial m_k}{\partial t} = -z_k \, exp\left(\frac{-E_k}{RT}\right) m_k \quad [5]$$

$\partial m_k / \partial t$ defines the mass loss rate of the active compound due to depletion in the reaction process. z_k is the pre-exponential constant, E_k is the activation energy of the reaction, and m_k is the normalised mass fraction of the active compound converted into gas for reaction '*k*'. *R* is the universal gas constant. Values for z_k, E_k and m_k must be determined experimentally using TGA. With Eqn. 5 it is assumed that all the chemical reactions are independent and first-order reaction rate processes. It is also assumed that the reaction rate is independent of the oxygen content of the fire atmosphere.

Voids develop in the coating due to the formation of volatiles within the hot, viscous melt of the decomposing intumescent material, and they cause the coating to swell. The void fraction increases with the mass fraction of volatiles (m_k) according to:

$$\omega = \frac{a_{ex} - \sum_k \gamma_k m_k}{a_{ex}} \quad [6]$$

where a_{ex} is the expansion factor of the coating, which must be determined experimentally.

Thermal analysis of the intumescent coating is solved using the FFD method in which the differential equations are solved at discrete points with respect to location and heating time; which is the same approach used to perform thermal analysis of the passive coating. Spatial grid

points are set up at different locations through the intumescent coating, and the model is solved at each of these locations for increasing heating times using a constant time step increment between successive iterations. As the coating expands due to the intumescent reactions, then the spacing between the grid points increases in the through-thickness direction according to:

$$x_{i+1,j} - x_{i,j} = a_{ex}(m_k)(x_{i+1,0} - x_{i,0}) \quad [7]$$

where $a_{ex}(m_k)$ is a variable expansion parameter.

The increase in coating thickness is determined by:

$$L_{ic}(t) = L_{ic,0} + \sum_i a_{ex}(m_k)\Delta x_0 \quad [8]$$

where L_{ic} is the intumescent coating thickness, which is dependent on the heating time. $L_{ic,0}$ is the initial thickness of the coating and the second term on the right-hand side of the equation calculates the thickness increase (in the x-direction) due to the reaction processes. The increase in coating thickness is calculated for increasing heating time (t).

Thermal Modelling of Fibreglass Laminate Substrate

The modelling approach out-lined above for the passive and intumescent coatings is coupled to thermal modelling of the fibreglass laminate substrate in the second stage of the analysis (refer to figure 1). This step of the analysis assumes that heat conducted from the back surface of the passive or intumescent coating flows directly into the laminate. It is assumed that no heat loss occurs across the coating/laminate boundary.

The increase in temperature of the laminate with increasing exposure time to this heat flux is calculated using the decomposition model for organic materials developed by Henderson et al. [24]:

$$\left[\frac{\partial T}{\partial t}\right]_{ls} = \frac{\left[\frac{\partial}{\partial x}\left(k_{c,x}^{ls}(T)\frac{\partial T}{\partial x}\right) - \dot{M}_G \frac{\partial}{\partial x}h_G - \rho\frac{\partial m_{ls}}{\partial t}(Q_P + h_C - h_G)\right]}{\left[\rho_{ls}(T).C_p^{ls}(T)\right]} \quad [9]$$

where the superscript or subscript '*ls*' refers to the laminate substrate. The thermal conductivity of the laminate ($k_{c,x}^{ls}$) is temperature dependent, and must be measured. ρ_{ls} and C_p^{ls} are the density and specific heat capacity of the laminate, respectively, and both properties are also temperature dependent. $\dot{M}_G$ and h_G are the mass flux and enthalpy of volatile gases produced by decomposition of the polymer matrix. Q_P and h_c are the heat of decomposition and enthalpy of the polymer matrix, and the reaction process is assumed to be endothermic. It is also assumed the glass fibre reinforcement is thermally inert, and does not release or absorb thermal energy due to reaction or phase changes.

The mass loss rate of the polymer matrix due to decomposition is assumed to occur via a single-stage reaction process that is described using the Arrhenius relationship:

$$\frac{\partial m_{ls}}{\partial t} = -z_{ls}\, exp\left(\frac{-E_{ls}}{RT}\right)m_{ls} \quad [10]$$

z_{ls} and E_{ls} are the pre-exponential factor and activation energy of the decomposition reaction of the polymer matrix, respectively, and these values must be measured using TGA of the polymer.

m_{ls} is the normalised mass fraction of the laminate converted into volatiles, and this is also determined by TGA.

Mechanical Modelling of Fibreglass Laminate Substrate

The final step to the modelling involves calculating the mechanical softening and failure of the laminate substrate when loaded in compression or tension. This part of the model is fully explained by the authors for the compression [10] and tension [11] load conditions, and therefore is only briefly out-lined in this section.

The mechanical analysis involves calculating the reduction in strength at different spatial locations across the load-bearing section of the laminate substrate based on the local temperature (which is calculated using Eqn. 9). The local compressive and tensile strengths of the laminate at any location and time are dependent on the local temperature. The local compressive strength is assumed to be dependent on the local temperature according to:

$$\sigma(T) = \left(\frac{\sigma_o + \sigma_r}{2} - \frac{\sigma_o - \sigma_r}{2} tanh(\Phi(T - T_k)) \right) R_s(T)^{n^*} \quad [11]$$

The first term on the right-hand side accounts for reversible softening caused by glass transition transformation of the polymer matrix from the 'glassy' to 'rubbery' states. The second term $R_s(T)^{n^*}$ accounts for permanent weakening due to decomposition of the polymer matrix. This term defines the strength loss of the laminate caused by matrix decomposition, with n^* being an empirical power-law factor. σ_o and σ_r are the strengths of the laminate at room temperature and in the fully softened condition, respectively. Φ is a material constant defining the temperature range over which the strength is reduced. T_k is the glass transition temperature defined by 50% strength loss.

Equation 11 is used to calculate the reduction to the compression strength of the laminate substrate due to thermal softening and decomposition. Compression softening of the laminate is dependent entirely on softening of the polymer matrix whereas tensile softening is controlled by both matrix softening and fibre softening.

Tensile strength loss is determined mostly by the reduction to the failure stress of the glass fibre reinforcement in the laminate. Glass fibre strength loss occurs at higher temperatures than matrix softening and is a time-dependent process. Calculating the reduction in glass fibre strength as a function of temperature and heating time and the reduction in matrix strength as a function of temperature is described by Feih et al. [11,25]. Using modified rule-of-mixtures analysis that combines the strengths of the glass fibres and polymer matrix at any location in the through-thickness direction of the laminate, then the local tensile strength at this point is calculated using [11]:

$$\sigma_T(T,t) = \Psi(T) V_f \sigma_f(T,t) + (1 - V_f)\sigma_m(T) \text{ with } \Psi \leq 1 \quad [12]$$

where Ψ is the load transfer factor to account for thermal softening of the polymer matrix, V_f is the fibre volume content, σ_f is the glass fibre strength (which is a function of temperature and heating time), and σ_m is the matrix strength which is dependent on the temperature. The determination of Ψ and σ_f is described by Feih et al [11].

Once the residual compressive and tensile strengths are calculated at many locations across the load-bearing section of the laminate substrate, the bulk (average) compressive or tensile strength is determined by averaging the local strength values using:

$$\sigma_{av} = \frac{1}{L_{ls}} \int_{0}^{L_{ls}} \sigma(x) dx \qquad [13]$$

where Simpson integration with 50 locations in the through-thickness direction of the laminate is used.

The model applies a strength-based criterion to define when the laminate substrate protected with a passive or intumescent coating will fail under static loading while heated from one side by fire. Compressive or tensile failure is assumed to occur when the average strength (σ_{av}) is reduced to the compressive or tensile stress applied to the laminate. The time for the average strength of the laminate to decrease to the applied stress value is taken to be the failure time. At this point it is assumed that all of the plies in the through-thickness direction fail at the same time. It is assumed therefore that progressive failure from the hot (front) surface towards the cooler (back) surface of the laminate substrate does not occur.

It is further assumed in the analysis of both the compression and tensile strengths that the coating is not structural and does not contribute to the strength properties. It is also assumed that heat-induced damage (e.g. delaminations, matrix cracks, fibre/matrix interfacial cracking) and visco-elastic creep softening of the fibres or matrix do not affect the strength properties, even though they are known to reduce the mechanical properties [18,27].

3 MATERIALS AND EXPERIMENTAL METHODS

3.1 Passive and Intumescent Coated Fibreglass Laminates

Fire structural tests were performed on flat fibreglass laminate substrate protected with a passive or instumscent coating to determine the numerical accuracy of the modelling approach for calculating the failure temperature and time. The configuration of the specimens is shown schematically in figure 2, with the coating applied over the surface of the laminate which is exposed to the simulated fire in the experimental tests. The laminate was reinforced using plain woven E-glass fabric with an areal density of 800 g/m^2 and weave pattern of 1 warp tow (0^o fibre direction) x 1 weft tow (90^o fibre direction). The fabric layers were arranged in the cross-ply [0/90] pattern. The polymer matrix was a commercial vinyl ester resin (Derakane 411-350; Ashland Composite Polymers) which was free of fire retardants. The substrate was made using the vacuum bag resin infusion process, and then cured under ambient conditions followed by an elevated temperature post-cure (80ºC for two hours). The fibre volume content was 55%. The 0^o fibres were aligned in the direction of compression and tension loading of the laminate in the structural fire test, which is described below. The thermal and mechanical properties of the laminate are given by Feih et al. [12].

The passive coating applied to the laminate substrate consisted of silicate filaments held together with an inorganic binder. The fibres are stable to around 1300°C, which is above the temperatures used in the fire structural test to assess the accuracy of the model. Insulation blankets with an average fibre density of 96 kg/m^3 and thickness of 13 and 25 mm were attached to the fire exposed surface of the laminate specimens. The thermal properties of the insulation material (k^{pc}, C_p^{pc}) are dependent on the temperature according to:

$$k_x^{pc} = 1.48\text{x}10^{-7}T^2 + 1.79\text{x}10^{-4}T + 1.29\text{x}10^{-2} \qquad [14]$$

and

$$C_p^{pc} = -1.17\text{x}10^{-4}T^2 + 0.416T + 776.4 \qquad [15]$$

The passive coating was bonded to the laminate substrate using high-temperature ceramic-based adhesive.

The intumescent coating (Zero Inc., Type FS2002) having a thickness of 5 mm was applied over the laminate substrate. The chemical composition, thermal conductivity and specific heat capacity properties of the intumescent material in the virgin and charred conditions are given by Asaro et al. [27]. The thermal and physical properties of the intumescent material are given in table 1. The intumescent coating was applied as a paste directly onto the laminate surface and bonded during drying at room temperature.

3.2 Structural Fire Testing

The accuracy of the model was assessed using temperature and time-to-failure values measured using a structural fire test method. Feih et al. [12] give a complete description of the test procedure, and therefore it is only briefly described here. The test basically involves applying a constant compression or tension load to a flat laminate specimen while heated from one-side at a constant heat flux. Tests were performed on the uncoated woven E-glass/vinyl ester laminate and the same laminate protected with the passive or intumescent coatings.

A constant compression or tension load was applied axially to the specimen using a 250 kN MTS machine. Load was applied parallel to the warp tow direction to the woven fibreglass reinforcement in the laminate specimens. Compression tests were performed at static compression loads between 10% and 90% of the Euler buckling stress of the fibreglass laminate specimen at room temperature (which was 21 MPa). Tension tests were performed at between 10% and 90% of the tensile failure stress of the laminate at room temperature (about 460 MPa).

The compression substrate specimens were 50 mm wide, 9 mm thick and 470 mm long between the loading points. The specimens were not restrained along their sides and therefore were free to buckle when their buckling load dropped below the applied compression load. The tension specimens were 50 mm wide, 9 mm thick and 730 mm long. When under load, the compression and tension specimens were exposed to a constant heat flux radiated from a 5 kW cone-shaped electric heater. A 100 mm long section at the centre of the compression and tension specimens was exposed to the heat flux while the remaining sections of the specimens were insulated to avoid heating. Localised heating of the central region of the specimens was performed to avoid warming of the grips and load cell of the MTS machine, which can affect the accuracy of the experimental results.

The specimen and heater were both oriented in the vertical direction, and spaced 25 mm apart. Fire structural tests were performed at heat fluxes of 25 and 50 kW/m^2, which heated the coated surface to about 400 and 650^oC, respectively. K-type thermocouples with a diameter of 1.5 mm were placed on the heated and unheated surfaces as well as embedded within the specimens. The thermocouple was embedded by inserting into a drilled hole from the side of the laminate. Specimens containing embedded thermocouples were used solely for temperature measurements, and were not used in structural testing because the hole can reduce the failure strength. The thermocouples were connected to a multi-channel data logger (DataTaker DT85) that recorded to temperature readings over the course of the fire structural tests.

The passive coating showed no obvious signs of thermal degradation during fire structural testing whereas the intumescent coating decomposed into char and increased in thickness. Figure 3 shows the effects of exposure time and heat flux on the thickening of the intumescent coating, which was measured from video images recorded during heat exposure. The time taken for the compression-loaded specimen to fail by micro-buckling or the tension-loaded specimen to fail by rupture while exposed to the constant heat flux was recorded. This failure time value was used to validate the model for different load and heat flux conditions.

4 RESULTS AND DISCUSSION

This section compares the temperature profiles, failure temperatures and failure times of the unprotected and coated fibreglass laminates calculated using the model against experimental values measured in the fire structural tests. This comparison is used to assess the numerical accuracy of the model.

An important step to the model is the calculation of the temperature in the fibreglass laminate with fire surface protection. It is essential that the coating temperature is accurately calculated using the model because it determines the softening, decomposition and failure of the underlying laminate substrate. The accuracy of the model was assessed by comparing the calculated and measured temperatures for the unprotected and coated laminates when exposed to one-sided radiant heating. Figure 4 presents temperature-time curves for the unprotected laminate and the laminate with the passive coating (25 mm thick) and intumescent coating (final thickness of ~26 mm) when exposed to the heat flux of 50 kW/m^2. The symbols are the experimental temperatures measured using thermocouples attached to the heated and back face surfaces and embedded within the specimen. The temperatures for the laminate without insulation were determined at the heated surface, mid-thickness point, and back surface of the specimen. The temperatures for the insulated specimens were determined at the heated coating surface, interface between the coating and laminate, and back surface of the laminate substrate. Equations 2 and 3 were used to calculate the temperatures of the passive and intumescent coatings, respectively. The solid lines are the theoretical temperatures calculated using the model at the same locations measured using the thermocouples. Figure 4 shows that the model predicted the initial heat-up rate and temperature profiles at different locations through the material with good accuracy at the heat flux of 50 kW/m^2. Similar agreements were found for the lower heat flux of 25 kW/m^2.

The model was also validated by comparing the calculated and measured failure times of the laminate protected with the passive or intumescent coating under in-plane compression or tension loading. Figure 5 shows the effect of applied compressive stress on the failure time of the laminate with or without a fire protective coating when exposed to the heat flux of 50 kW/m^2. Compressive failure in all cases occurred by localised microbuckling of the load-bearing plies within the heated zone of the laminate specimen, as shown in figure 6. Microbuckling occurred due to visco-plastic shear softening of the polymer matrix when heated near the glass transition temperature, which resulted in out-of-plane rotation of the load-bearing plies and delamination cracking between the plies [10].

Figure 5 shows that the failure times for the laminate protected with the passive or intumescent coatings were much longer than the unprotected material, and this was due to the thermal insulation provided by the coating. In this study it was found that the failure times for the laminate protected with the passive coating were much longer than the intumescent coating, and at applied compression stress values below ~10 MPa the laminate with the passive coating did not fail. The better protection provided by the passive coating was due to it providing greater insulation than the intumescent coating (as shown in figure 4 by the passive coated laminate having a lower temperature than the intumescent coated material at the coating/laminate interface and at the back face of the laminate substrate). The thermal conductivity of the passive coating over the range of test temperatures (calculated using eqn. 14) was lower than that of the intumescent material (table 2). It is also possible that some oxidation of the intumescent char occurred which would lower the heat insulation to the laminate substrate.

The curves in figure 5 show the calculated increase in the failure times for the unprotected and coated laminates with decreasing compressive stress, and the agreement with most of the experimental times is reasonable. In several instances the agreement between the calculated and measured failure times is poor, most notably at the lowest applied stresses when the times are the longest. This inaccuracy is attributed to the mechanical model not analysing for visco-elastic

creep of the laminate substrate, which is known to be a controlling softening process for long loading times at temperatures close to and above the glass transition temperature [5-7]. Furthermore, the mechanical model does not consider the influence of heat-induced damage, such as delaminations, on the failure time. The testing also revealed that failure occurred progressively across the load-bearing section of the laminate, rather than uniformly as assumed in the model.

The effect of applied tensile stress on the failure times of the unprotected and coated laminates is shown in figure 7 for the heat flux of 50 kW/m^2. There is little data for the laminate with the passive coating because the specimens only failed when the applied stress was very high. The high thermal insulation provided by the passive coating stopped tensile failure for most of the load conditions. Regardless of whether the laminate was unprotected or protected with a surface coating, failure always occurred by tensile rupture involving breakage of the load-bearing plies, with partial or complete decomposition of the polymer matrix. The typical appearance of a specimen that failed in tension is shown in figure 8, and the polymer matrix is completely removed exposing the woven glass reinforcement. Such severe matrix decomposition was not observed with the compression specimens (figure 6), that failed within shorter times and therefore at lower temperatures. Figure 7 also shows that the tension failure times were extended by the passive and intumescent coatings, and as with the compression load case this was due to the insulating effect provided by these coating systems. Again, in the study the passive coating extended the failure times more than the intumescent coating.

The curves in figure 7 show the calculated increase in the failure times of the laminate with and without the coating when the applied tensile stress was reduced. The model predicts the general trend of increasing failure time with decreasing heat flux and stress level, however the agreement with the experimental data is in most cases not exact as the model does not consider the statistics of single fibre failure but instant considers simultaneous rupture of all the fibres. Again, the difference between the calculated and measured failure times becomes greater the longer the time. In other words, the agreement is better for shorter times (often <1000 s) than for the longer times (> 1000 s).

The numerical accuracy of the model was assessed further using the back face temperature of the laminate substrate when failure occurred under compression or tension loading. The back face temperature is often used to quantify the fire resistance of composite structures subjected to one-sided fire attack [18]. Figure 9 compares the calculated and measured back face temperatures for the unprotected and coated laminates. The back face temperatures were determined at the time at which the laminate failed in compression or tension. The closer the data points are to the line (which has a gradient of unity) then the closer is the agreement between the calculated and measured back face temperatures. There is good agreement between the theoretical and experimental temperatures in most cases, with the Pearson product-moment correlation coefficient (ρ_a) between the calculated and measured temperatures being 0.97 and 0.99 for the compression and tension load conditions, respectively. Figure 9 also shows the decomposition temperature of the polymer matrix of the laminate, which starts at ~380^{o}C. It is seen that the failure temperatures were always below the back surface decomposition temperature for both the unprotected and coated laminates subjected to compression loading. However, the laminate was able to withstand tension loading at temperatures above that required to cause complete decomposition of the polymer matrix, and this was due to the capacity of the glass fibres to carry the applied load after the matrix had decomposed.

Figure 10 presents a comparison between the calculated and measured failure times for the laminate with and without an insulation coating when subjected to combined one-sided heating at heat fluxes of 25 and 50 kW/m^2 and loading under compression and tension. As with the plots in figure 9, the closer the data point resides to the line then the closer is the agreement between

the calculated and measured failure times. The agreement is best for relatively short failure times (less than ~1000 s) for both heat flux and load conditions. At longer failure times (above ~1000 s) the agreement is poor, with the model both over-predicting and under-predicting the measured failure times. Figure 10 gives the average Pearson correlation coefficient (ρ_a) and the Pearson correlation coefficients for short (<1000 s) and long (>1000 s) failure times, which are defined by $\rho_{<1000s}$ and $\rho_{>1000s}$, respectively. The Pearson correlation coefficient for short failure times ($\rho_{<1000s}$) is 0.96 and 0.93 for compression and tension loading, respectively. However, the correlation coefficient for long times is low (ρ_a ~ 0.75 for the two loading conditions). This implies that the numerical accuracy of the model is limited to short failure times, which occurs for high heat flux and/or high load conditions.

The agreement between the calculated and measured failure times shown in figure 10 is worse than for the calculated and measured failure temperatures given in figure 9. It is believed the inaccuracy of the mechanical model arises from several simplifying assumptions, such as ignoring temperature-time-dependent deformation (i.e. creep of the polymer matrix and stress rupture of the glass fibres) which is known to be a controlling process in the failure of laminates at long loading times [5-7,11,27] and ignoring the influence of heat-induced damage such as matrix cracks and delaminations which weaken the laminate [18,27]. An important factor contributing to the numerical inaccuracy of the model is the assumption that failure occurs uniformly across the load-bearing section of the laminate at a well-defined time/temperature. During testing it was observed that the laminate specimens did fail catastrophically, but instead failed progressively by microbuckling (under compression) or tensile rupture (under tension) of individual plies starting from the hot face where the material is weakest. It is believed that plies fail sequentially across the load-bearing section of the laminate until the average material strength drops below the applied stress when the remaining plies fail together. Accurately capturing these and other processes is needed to improve the numerical accuracy of the coupling components of the model for predicting the survival time of uncoated and coated fiberglass laminates exposed to fire.

5 CONCLUSIONS

This paper has presented a thermal-mechanical model to analyse the fire structural survivability of fibreglass laminates with passive or intumescent coating systems. The model combines heat transfer analysis of the coating, heat transfer and decomposition analysis of the laminate substrate, and mechanical analysis of the laminate to predict the backface failure temperature and failure time. The numerical accuracy of the model was assessed using failure temperature and time data obtained from fire structural tests performed on an unprotected woven E-glass/vinyl ester laminate and the laminate with a passive coating (ceramic fibre mat) and organic intumescent coating. The model was capable of predicting the backface failure temperature of the uncoated and coated laminates when exposed to heat fluxes of 25 and 50 kW/m^2, which heated the fire exposed surface to about 400 and 650^oC, respectively. The model was also able to estimate the failure times with reasonable accuracy when compression and tension failure occurred within a relatively short heating period (less than ~1000 seconds). At longer times, however, the model was unable to reliably predict the failure time. This inaccuracy is attributed to several simplifying assumptions of the mechanical analysis. Further development of the model with consideration to factors such as creep, heat-induced damage and progressive failure is essential to improve the predictions of structural survivability time of insulated fibreglass laminates subjected to fire attack.

ACKNOWLEDGMENTS

The authors acknowledge the Cooperative Research Centre for Advanced Composite Structures Limited (CRC-ACS) for its support of their work, which has been carried out as part

of the CRC-ACS research program. The authors thank Assoc Prof Brian Lattimer (Virginia Tech), Dr Greg Griffin (RMIT University) and Zenka Mathys (Defence Science and Technology Organisation) for discussions and other assistance with this work. The authors also thank Peter Tkatchyk (RMIT University) and Sarina Russo (Defence Science and Technology Organisation) for technical assistance. The study was funded by the United States Office of Naval Research (Grant No. N00014-07-10514) under the direction of Dr L. Couchman.

REFERENCES

1. McManus HL, Springer GS. High temperature thermo-mechanical behaviour of carbon-phenolic and carbon-carbon composites, I. Analysis. J Comp Mat. 1992; 26: 230-255.
2. Dao M, Asaro RJ. A study on failure prediction and design criteria for fibre composites under fire degradation. Comp. 1999; 30A: 123-131.
3. Krysl, P, Ramroth WT, Steward LK, Asaro RJ, Finite element modeling of fibre reinforced polymer sandwich composites exposed to heat. Int J Num Meth Eng. 2004; 61: 49-68.
4. Key CT, Lau J. Constituent based analysis of composite materials subjected to fire conditions. Comp. 2006; 37A: 1005-1014.
5. Bausano JV, Lesko JJ, Case SW. Composite lifetime during combined compressive loading and one-sided simulated fire exposure: characterization and prediction. Comp. 2006; 37A: 1092-1100.
6. Boyd SE, Lesko JJ, Case SW, Compression creep rupture behavior of a glass/vinyl ester composite laminate subject to fire loading conditions. Comp Sci & Tech 2007: 67; 3187-3195.
7. Boyd SE, Case SW, Lesko JJ. Compression creep rupture behavior of a glass/vinyl ester composite subject to isothermal and one-sided heat flux conditions. Comp. 2007; 38: 1462-1472.
8. Gibson AG, Wright PNH, Wu Y-S, Mouritz AP, Mathys Z, Gardiner CP. The integrity of polymer composites during and after fire. J Comp Mat. 2004; 38: 1283-1308.
9. Gibson AG, Wu Y-S, Evans JT, Mouritz AP. Laminate theory analysis of composites under load in fire. J Comp Mat. 2006; 40: 639-658.
10. Feih S, Mathys Z, Gibson AG, Mouritz AP. Modelling the compression strength of polymer laminates in fire. Comp. 2007; 38A: 2345-2365.
11. Feih S, Mathys Z, Gibson AG, Mouritz AP. Tensile strength modelling of glass-fibre polymer composites in fire. J Comp Mat. 2007; 41: 2387-2410.
12. Feih S, Mathys Z, Gibson AG, Mouritz AP. Modelling the tension and compression strengths of polymer laminates in fire. Comp Sci Tech. 2007; 67: 551-564.
13. Easby RC, Feih S, Konstantis C, La-Delfa G, Urso Miano V, Elmughrabi A, Mouritz AP, Gibson AG. A failure model for phenolic and polyester pultrusions under load in fire. Plas Rubb & Comp. 2007; 36: 379-388.
14. Bai Y, Vallée T, Keller T. Modeling of thermal responses for FRP composites under elevated and high temperatures. Comp Sci & Tech. 2008; 68: 47-56.
15. Bai Y, Vallée T, Keller T. Modeling of mechanical responses for FRP composites in fire. Comp. 2009; 40A: 731-738.
16. Gu P, Doa M, Asaro J. Designing polymer matrix composite panels for structural integrity in fire. Comp. Struct. 2008;84:300-309.
17. Gu P, Asaro J. Structural stability of polymer matrix composite in fire. Marine Struct., 2009;22:354-372.
18. Mouritz AP, Gibson AG. Fire Properties of Polymer Composite Materials, Springer, Dordrecht, 2006.
19. Sorathia U, Beck C. Fire protection of glass/vinyl ester composites for structural applications, Proceedings of the 41st International SAMPE Symposium, 1996, pp. 687-697.
20. Mouritz AP, Mathys Z. Post-fire mechanical properties of glass-reinforced polyester composites, Comp Sci & Tech. 2001; 61: 475-490.
21. Xie W, DesJardin PE. An embedded upward flame spread modeling based on 2D direct numerical simulation. Comb. & Flame, 2009; 156: 522-530.

22. Xie W, DesJardin PE. A level set embedded interface method for conjugate heat transfer simulation of low speed 2D flows. Comp & Fluids. 2008; 37: 1262-1275.
23. Griffin GJ. The modeling of heat transfer across intumescent polymer coatings. J Fire Sci. 2010; 28: 249-277.
24. Henderson JB, Wiebelt JA, Tant MR. A model for the thermal response of polymer composite materials with experimental verification. J Compos Mater 1985; 19: 579-595.
25. Feih S, Manatpon K, Mathys Z, Gibson AG, Mouritz AP. Strength degradation of glass fibres at high temperature. J Mat Sci., 2009;44:392-400.
26. Mouritz AP, Feih S, Kandare E, Mathys Z, Gibson AG, Des Jardin PE, Case SW, Lattimer BY, Review of fire structural modelling of polymer composites, Comp, 2009;40A:1800-1814.
27. Asaro RJ, Lattimer BY, Mealy C, Steele G. Thermo-mechanical performance of a fire protective coating for naval ship structures. Comp. 2009; 40A: 11-18.

Table 1: Property data for intumescent coating.

Property	**Material state**	**Value**	**Reference source**
Thermal conductivity (W/m °C)	Virgin Intumesced Charred	0.4 $3.00 \times 10^{-4}T + 0.1$ $3.00 \times 10^{-4}T + 0.1$	27 27 27
Specific heat capacity (J/kg °C)	Virgin Intumesced Charred	2200 1.5T + 3000 2.0T + 2800	27 27 27
Original thickness (mm)	-	5.00	27
Density (kg/m^3)	Virgin	1392	27
Heat of decomposition (J/kg)	-	0.24×10^6	27
γ_k z_k (s^{-1}) Ea_k (kJ/mol)	Melting	0.061 1.71×10^5 56.4	
γ_k z_k (s^{-1}) Ea_k (kJ/mol)	Intumesced	0.151 1.06×10^4 66.4	
γ_k z_k (s^{-1}) Ea_k (kJ/mol)	Char	0.268 5.50×10^6 122.9	

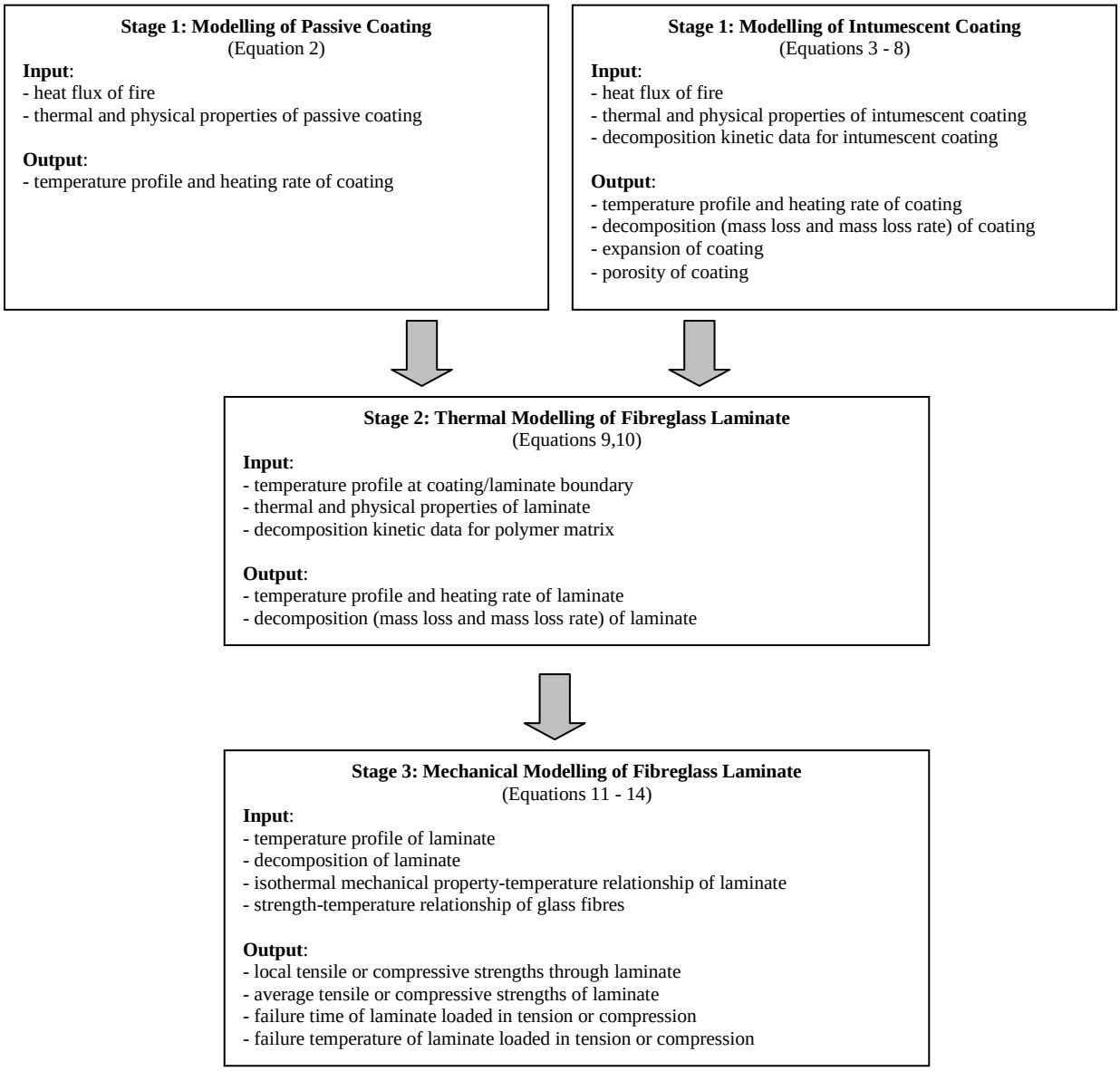

Figure 1. Summary flow-chart of the three-stage modelling approach to calculate the fire structural properties of fibreglass laminates with passive or intumescent insulation coating.

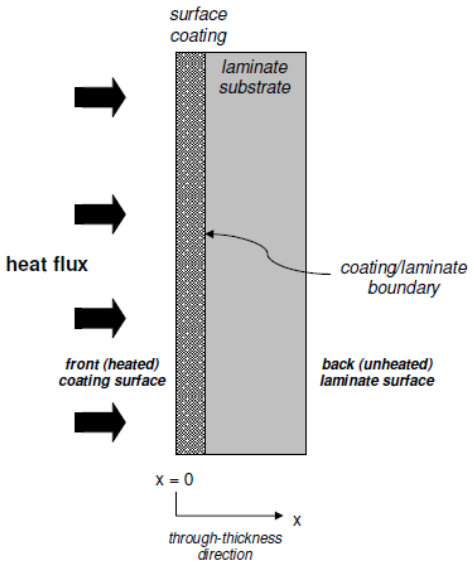

Figure 2. Representation of the laminate substrates protected with passive coating or intumescent coating.

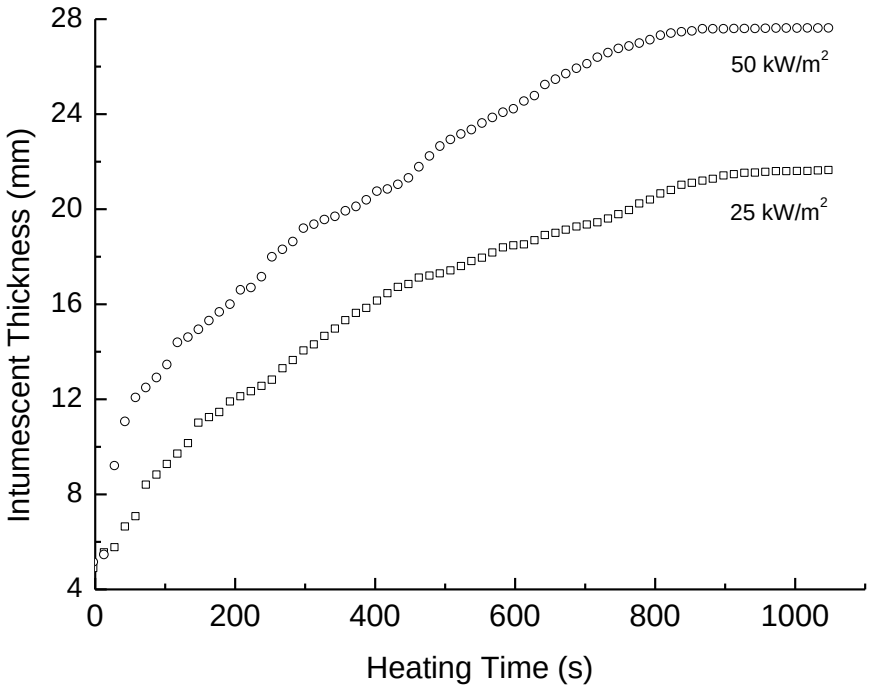

Figure 3. Effect of heating time on the thickness of the intumescent coating when exposed to the heat fluxes of 25 and 50 kW/m^2.

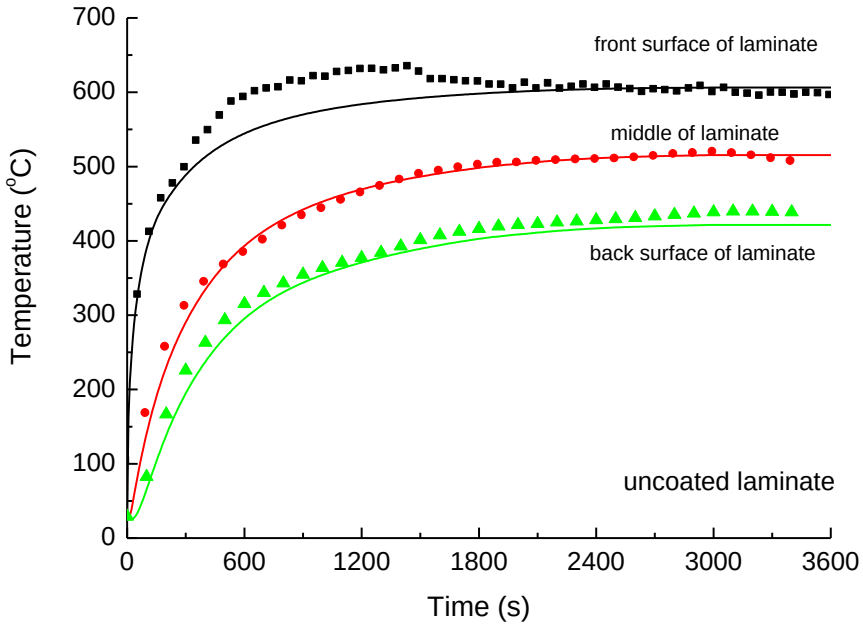
front surface of laminate
middle of laminate
back surface of laminate
uncoated laminate
Temperature (°C)
Time (s)
0
100
200
300
400
500
600
700
0
600
1200
1800
2400
3000
3600

(a)

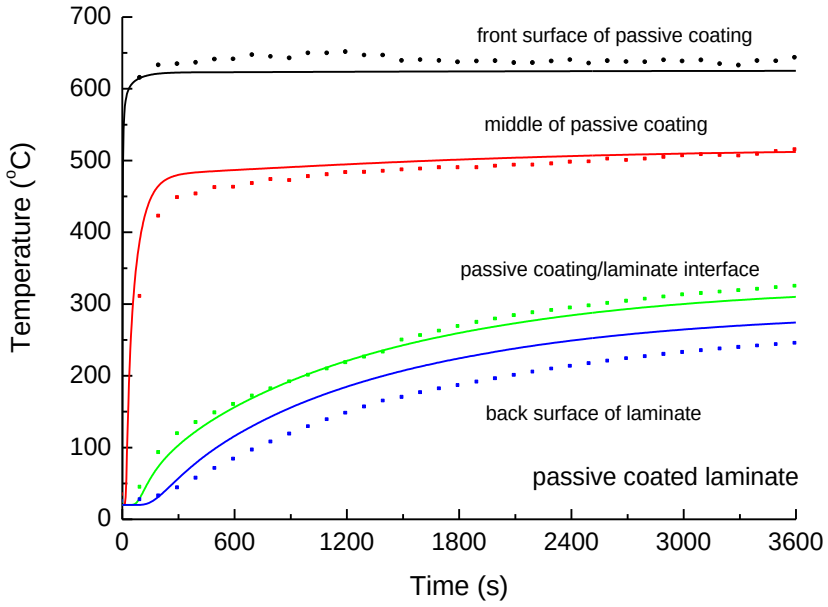
front surface of passive coating
middle of passive coating
passive coating/laminate interface
back surface of laminate
passive coated laminate
Temperature (°C)
Time (s)
0
100
200
300
400
500
600
700
0
600
1200
1800
2400
3000
3600

(b)

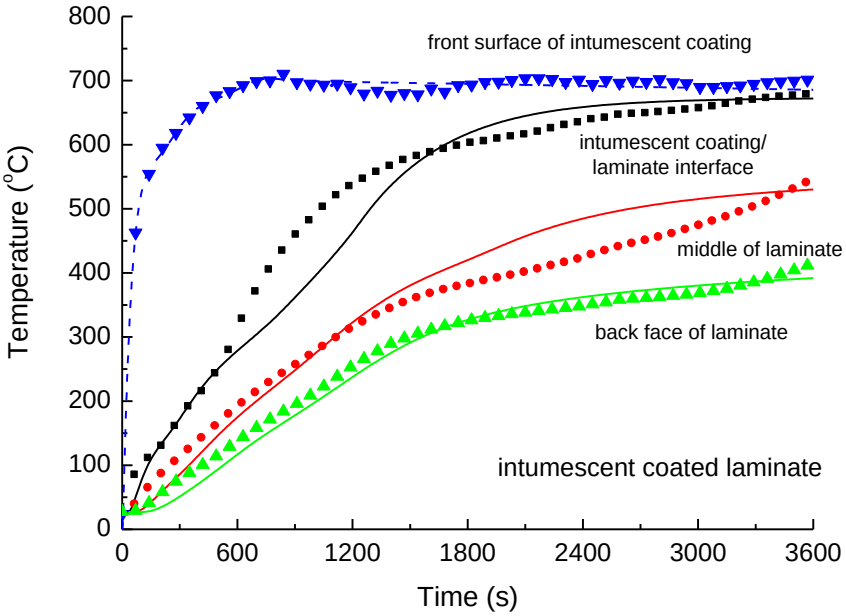

(c)

Figure 4. Temperature-time profiles determined at different locations in the (a) uncoated laminate, (b) laminate with the passive coating (25 mm thickness), and (c) laminate with the intumescent coating. The data points show the experimentally measured temperatures and the curves were calculated using the model. The incident heat flux was 50 kW/m^2.

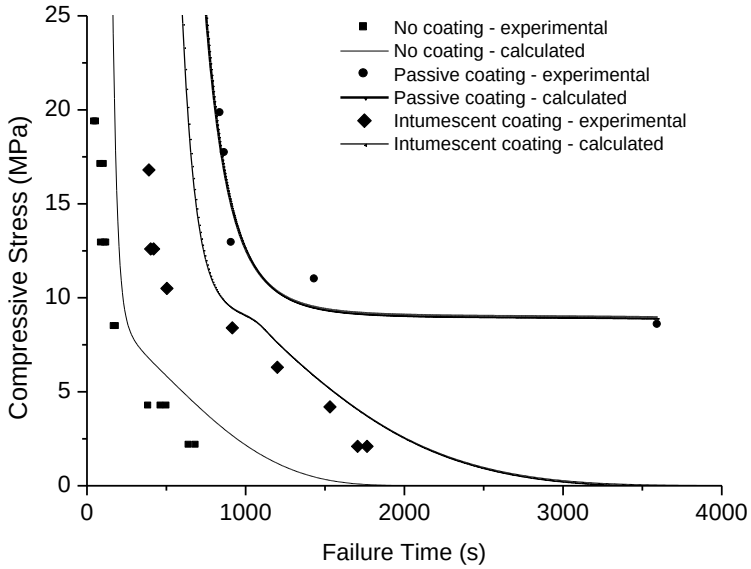

Figure 5. Effect of applied compression stress on the failure times of the laminate with or without fire protection coating. The data points show the experimental failure times and the curves were calculated using the model. The passive coating was 25 mm thick. The incident heat flux was 50 kW/m^2.

Figure 6. Compressive failure of the laminate during fire structural testing involved plastic microbuckling of the load-bearing plies and delamination cracking between the plies.

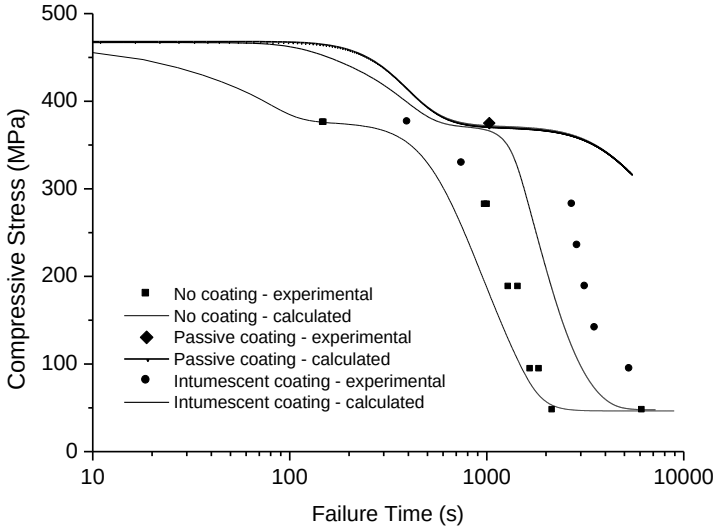

Figure 7. Effect of applied tension stress on the failure times of the laminate with or without fire protection coating. The data points show the experimental failure times and the curves were calculated using the model. The passive coating was 25 mm thick. The incident heat flux was 50 kW/m^2.

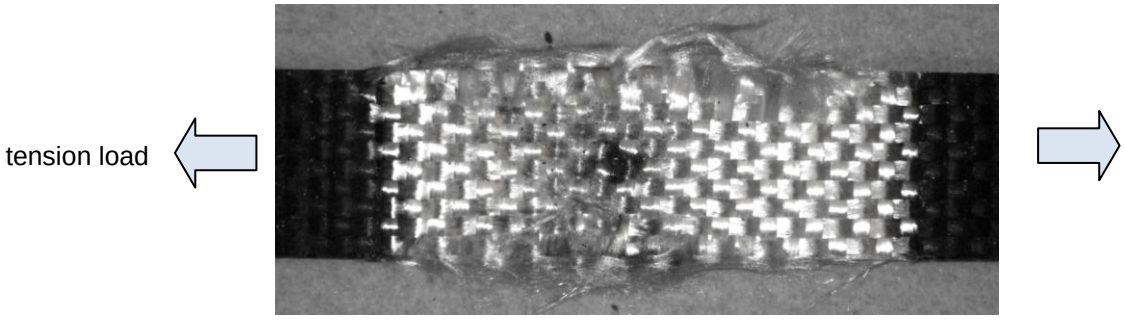

Figure 8. Tensile failure of the laminate during fire structural testing involved rupture of the load-bearing plies. The white region shows where the glass fibres have been exposed due to decomposition and vaporisation of the polymer matrix.

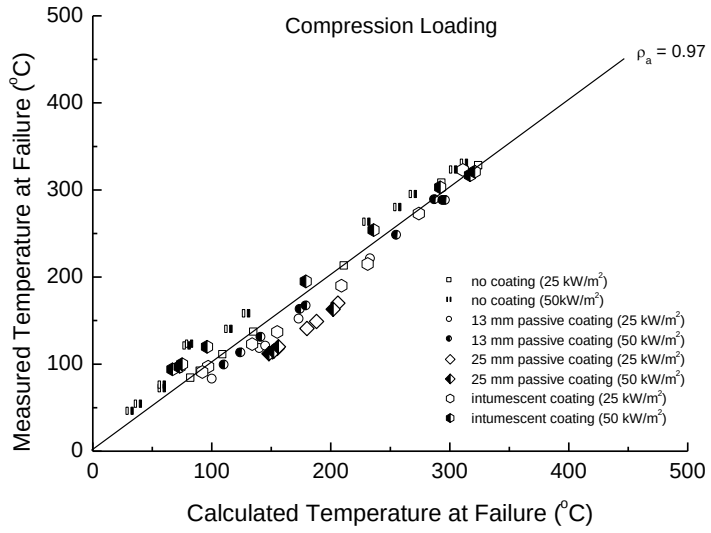

(a)

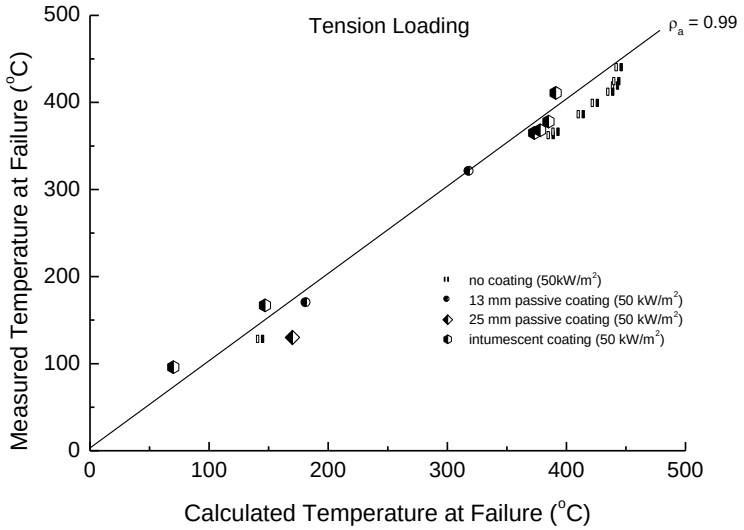

(b)

Figure 9. Comparison of the calculated and measured back surface temperatures at failure of the fibreglass laminate. (a) Compression loading. (b) Tension loading.

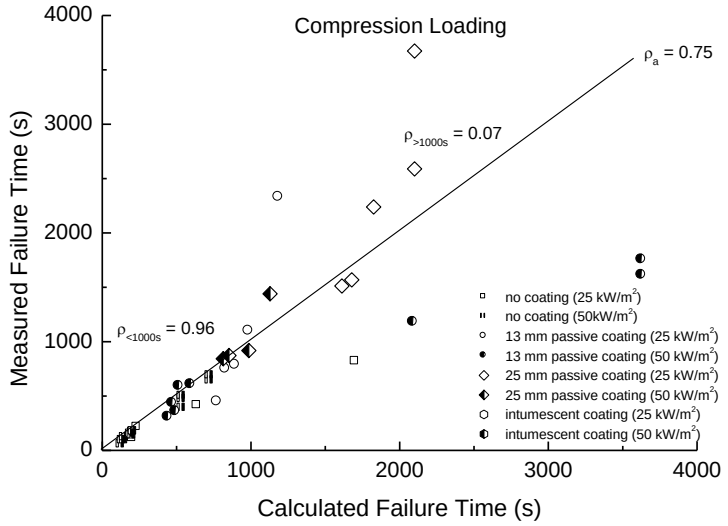

(a)

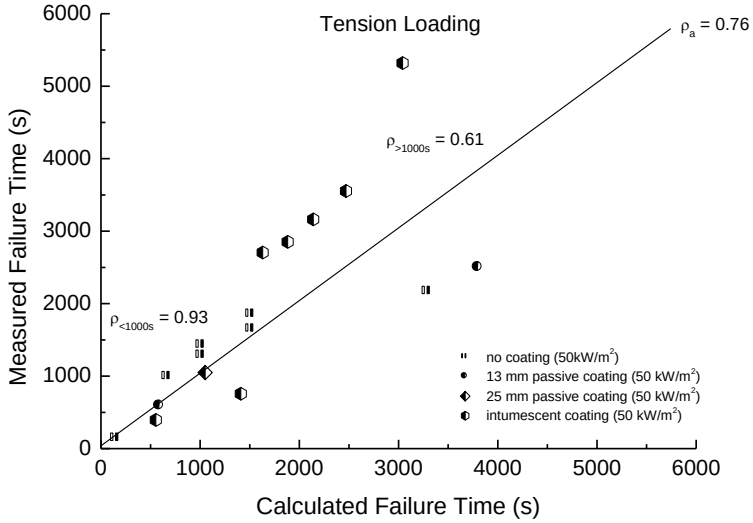

(b)

Figure 10. Comparison of the calculated and measured failure times at failure of the fibreglass laminate. (a) Compression loading. (b) Tension loading.